Improving Solar Wind Forecasting Models Over the Phase of Solar Cycle: Source Surface Height Optimization and Magnetogram Impact

Sandeep Kumar[1,4], Nandita Srivastava[1],
Dana-Camelia Talpeanu [2], Marilena Mierla [2,3], Elke D'Huys[3], Marie Dominique [3]

[1] Udaipur Solar Observatory, Physical Research Laboratory, Udaipur 313001, India
[2]Solar-Terrestrial Centre of Excellence—SIDC, Royal Observatory of Belgium, 1180 Brussels, Belgium
[3]Institute of Geodynamics of the Romanian Academy, Bucharest, Romania
[4]Discipline of Physics, Indian Institute of Technology Gandhinagar, India

Abstract

The operational solar wind velocity prediction models used by the community are based on the Potential Field Source Surface (PFSS) model of the magnetic field. Previous studies have suggested different values of source surface heights (R_{ss}) in the PFSS model at different phases of the solar cycle (SC). We investigate the necessity of optimizing the R_{ss} in the PFSS model in the context of its use in the popular Wang Sheeley and Arge (WSA) model for solar wind velocity prediction. We performed a study of 16 Carrington Rotations (CR) at different phases of the SC24 and SC25, using different types of magnetograms and WSA model parameters. Our results suggest that we can improve the model prediction by using different R_{ss} at different phases of SC and using zero-point corrected (ZPC) GONG maps. We further validate the superiority of ZPC maps over standard GONG maps by comparing the PFSS extrapolation with PROBA2/SWAP images at 174 Å.

PFSS and Solar Wind

The magnetic field from PFSS [7] model is used as an input in empirical solar wind models like Wang-Sheeley, Distance from Coronal Hole Boundary (DCHB) and the Wang-Sheeley-Arge [WSA; 1]. The main PFSS parameter is the height of the source surface (SS), and it is crucial for the extrapolation of the field above the photosphere. [3] also investigated the effects of changing the shape of the source surface from a sphere to an ellipsoid. The source surface height (R_{ss}) in the PFSS model, defines the upper boundary where the magnetic field lines are open and radial in the heliosphere. Previous studies conducted in the context of open flux measured at L1 using different magnetograms agree in terms of the relative changes in the best SS heights with the phase of the SC ([4] and references therein). One of the important aspects of R_{ss} optimization is in the context of the use of PFSS in solar wind velocity prediction models at L1.
In this work, we optimize R_{ss} in the PFSS model with the solar cycle phase to be used in the WSA model.

$$v_{sw}^{wsa}(f_s,\theta_b) = v_{slow} + \frac{v_{fast}-v_{slow}}{(1+f_s)^{\alpha}}\left(\beta - \gamma e^{-(\theta_b/w)^{\delta}}\right)^{3.5} \quad (1)$$

We evaluated the performance of the solar wind velocity prediction framework (PFSS+WSA+HUX) at L1 using different R_{ss}, on 16 Carrington Rotations (CRs) selected at different phases of SC24 and SC25 as shown in the Figure1.

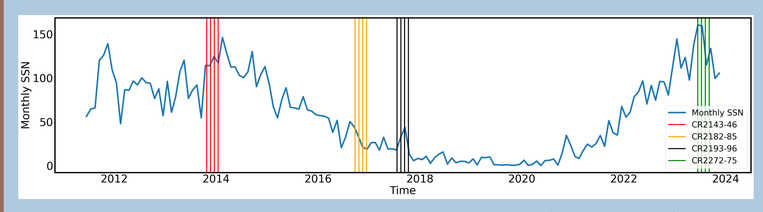

Figure1: Monthly sunspot numbers (blue line) plotted with time, indicating different phases of SC24 and SC25. The vertical lines mark the CRs selected for analysis in different phases of the solar cycle

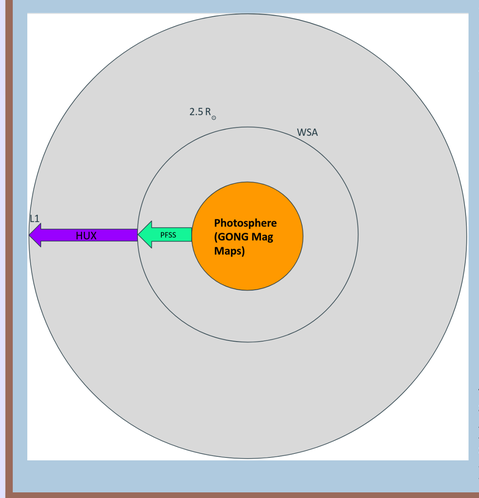

Figure 2: Framework to predict solar wind velocity at L1 and find the best R_{ss}.

Table 1. Parametric space used for WSA model.

Parameter	Range	No. of Points
V_{slow}	200-300 km s^{-1}	3 points
V_{fast}	600-800 km s^{-1}	5 points
α	0.1 to 0.3	6 points
β	1 to 1.75	4 points
w	0.01 to 0.05 radian	5 points
γ	0.6 to 1.0	3 points
δ	0.8 to 1.5	3 points

Acknowledgment: We acknowledge PROBA2 GI program, pfsspy, sunpy, GONG, ESA's PRODEX Programme.

Methodology

Predicting solar wind velocity at the L1 point for the 16 CRs and selecting the best R_{ss} among three choices, i.e., 2.0 $R_\odot$, 2.5 $R_\odot$, and 3.0 $R_\odot$, for each type of input magnetic map (hourly updated (HU) and full CR zero point corrected maps (ZPC) and full CR synoptic standard synoptic maps (STD), in the framework involves the following steps:

1. Calculate the magnetic field in the coronal domain, i.e., up to R_{ss}, using the PFSS. Use three different values of R_{ss} (2.0 $R_\odot$, 2.5 $R_\odot$, and 3.0 $R_\odot$), for each of the three different types of input synoptic magnetic maps.
2. Trace the magnetic field lines from the photosphere to create a map of open and closed field lines.
3. Trace the sub-Earth field lines from R_{ss} to the photosphere.
4. Utilize the WSA empirical velocity relation to estimate solar wind velocity profile at R_{ss}, based on the magnetic field line properties, using: (1) Default WSA parameters, (2) A parametric space of WSA parameters. Using parametric space involves a range of values of WSA parameters to arrive at a conclusion independent of the choice of parameters.
5. Extrapolate velocity estimates from the outer boundary of the coronal domain (R_{ss}) up to the L1 point using the HUX extrapolation [5](heliospheric domain) .
6. Apply the first three steps for each value of R_{ss}, with default WSA parameters and for parametric space (Table 1) for each type of magnetic map, and calculate the performance matrix defined by Pearson's correlation coefficient.

Results

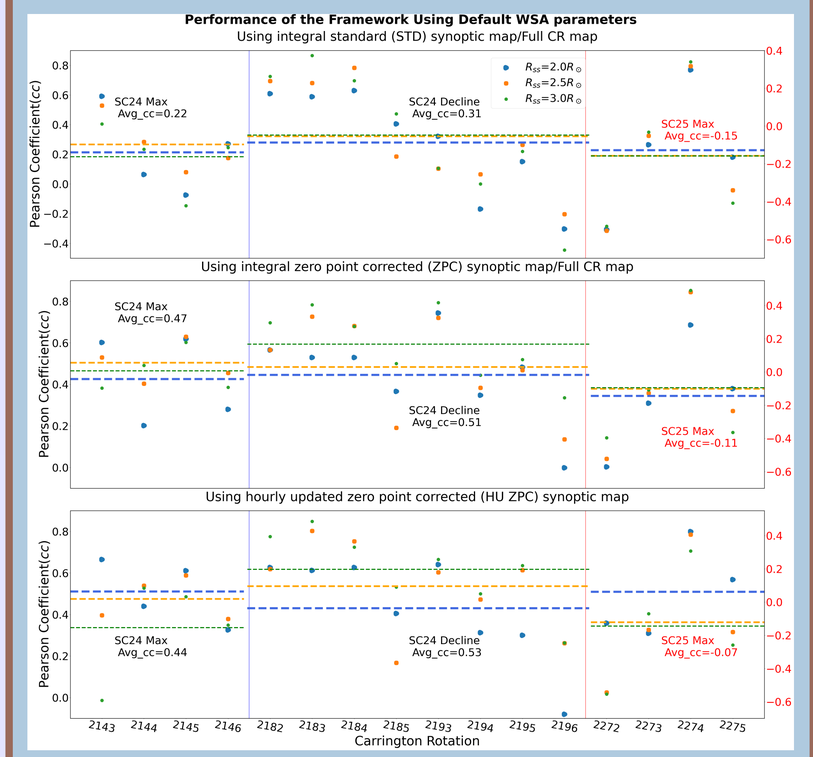

Figure 3: The performance of the framework (cc) for different CRs with different R_{ss} based on default WSA parameters. Horizontal dashed lines show the average performance in the respective phase for each R_{ss} and all CRs. The annotated value shows the average value of cc for each input map and SC phase for the three values of R_{ss}.

PFSS and SWAP Observations

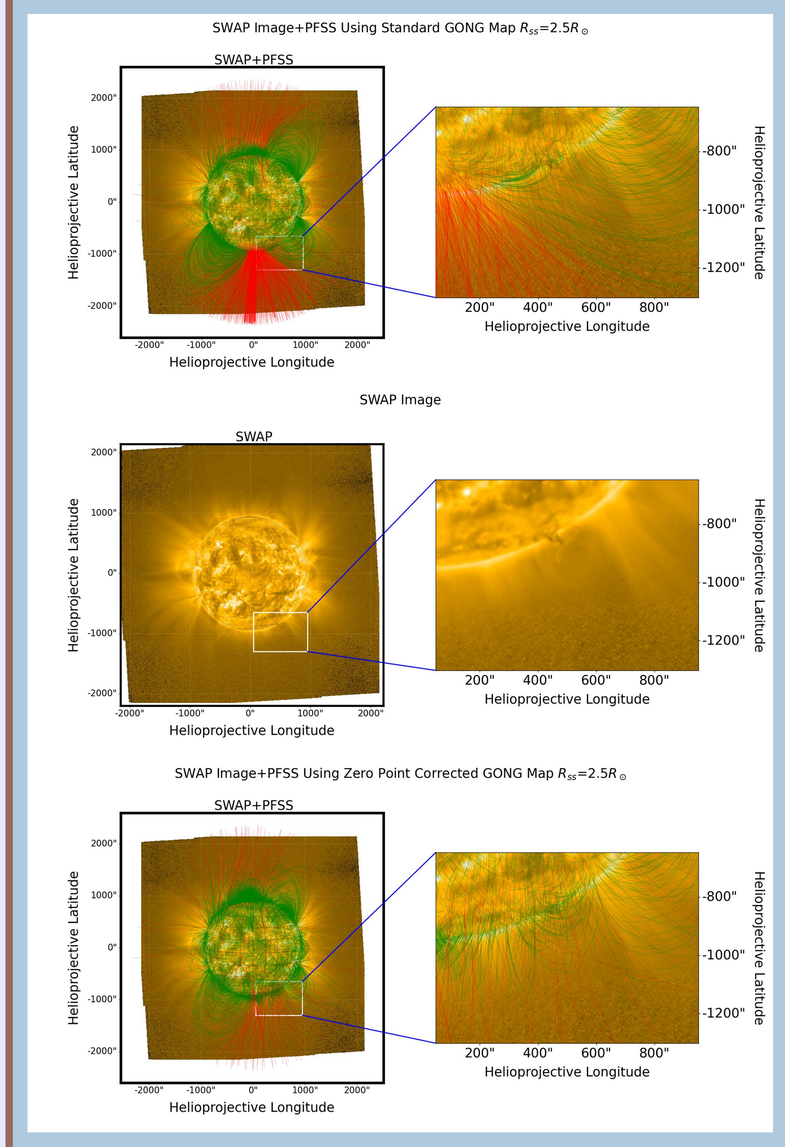

Figure 4: PFSS extrapolated magnetic field lines overlaid on PROBA2/SWAP [6, 2] images recorded on 7 August 2023, 20:37 UT. The top panel shows PFSS extrapolation with STD maps and the bottom panel with ZPC maps. The middle panel shows the SWAP image without PFSS extrapolation.

Conclusion

Our results suggest using a higher (3.0 $R_\odot$) and lower (2.0 or 2.5 $R_\odot$) surface height in the WSA model respectively during SC minimum and maximum, as compared to the conventional R_{ss} (2.5 $R_\odot$). We found substantial improvement in the performance of the solar wind forecasting framework while using zero-point-corrected magnetic maps compared to standard maps, which is further confirmed by the comparison of PFSS extrapolation with the EUV coronal observations of the Sun at 174Å obtained from the PROBA2/SWAP instrument.

References

[1] C. N. Arge, D. Odstrcil, V. J. Pizzo, and L. R. Mayer. Improved Method for Specifying Solar Wind Speed Near the Sun. In M. Velli, R. Bruno, F. Malara, and B. Bucci, editors, *Solar Wind Ten*, volume 679 of *American Institute of Physics Conference Series*, pages 190–193, Sept. 2003.
[2] J. P. Halain, D. Berghmans, D. B. Seaton, B. Nicula, A. De Groof, M. Mierla, A. Mazzoli, J. M. Defise, and P. Rochus. The SWAP EUV Imaging Telescope. Part II: In-flight Performance and Calibration. *Solar Physics*, 286(1):67–91, Aug. 2013.
[3] M. Kruse, V. Heidrich-Meisner, R. F. Wimmer-Schweingruber, and M. Hauptmann. An elliptic expansion of the potential field source surface model. *Astronomy And Astrophysics*, 638:A109, June 2020.
[4] L. Nikolić. On solutions of the pfss model with gong synoptic maps for 2006–2018. *Space Weather*, 17(8):1293–1311, 2019.
[5] P. Riley and R. Lionello. Mapping Solar Wind Streams from the Sun to 1 AU: A Comparison of Techniques. *Solar Physics Journal*, 270(2):575–592, June 2011.
[6] S. Santandrea, K. Gantois, K. Strauch, F. Teston, Proba2 Project Team, E. Tilmans, C. Baijot, D. Gerrits, Proba2 Industry Team, A. de Groof, G. Schwehm, and J. Zender. PROBA2: Mission and Spacecraft Overview. *Solar Physics Journal*, 286(1):5–19, Aug. 2013.
[7] K. H. Schatten and J. M. Wilcox. A model for interplanetary and coronal magnetic fields. *Solar Physics*, 1968.